

TG-FTIR analysis of co-combustion characteristics of oil shale semi-coke and corn straw

Hongpeng Liu¹  · Shishang Gong¹ · Chunxia Jia¹ · Qing Wang¹

Received: 5 April 2016 / Accepted: 19 July 2016 / Published online: 2 August 2016
© Akadémiai Kiadó, Budapest, Hungary 2016

Abstract TGA/DSC1 thermogravimetric analyzer and Fourier infrared spectrometric analyzer (FTIR) were used to conduct a series of combustion experiments using oil shale semi-coke, corn straw, and blends of the two. The results showed that the volatile initial precipitation temperature and ignition temperature of mixed samples are much lower than oil shale semi-coke, but it slightly higher than corn straw. The volatile initial precipitation temperature and ignition temperature of the mixed sample are increased with the increase in heating rate. When the heating rate is constant, the combustion process presents the trend to the low temperature; the peak value of the low-temperature section is high and intense release of volatile, thus improved combustion characteristics of the mixtures. Infrared spectral results are that: with increasing proportion of corn straw, A_{CO}/A_{CO_2} decreases gradually; the utilization rate of mixtures is improved. The value of A_{CO}/A_{CO_2} is minimum at the heating rate of 20 K min^{-1} , combustion effect of mixtures is best, and the burnout rate is highest. *RMS* and *MR* values are used to evaluate the mutual influence of the co-combustion process and the study showed that main effects of the interaction occurred in second, third and fourth stages, the second and third stages are the favorable effects, and the fourth stage is the adverse effect and when the mass ratio of the semi-coke and the corn straw is 7:3, the mutual influence is the largest and the beneficial effects. The model of distributed activation

energy is applied to analyze co-combustion kinetics of the blends. The results show that activation energy presents a rising tendency during the impelling of reaction, which is unanimous to the change law of DTG and FTIR curves. The results can provide reference for efficient combustion of oil shale semi-coke and corn straw.

Keywords Oil shale semi-coke · Corn straw · Co-combustion · Mutual influence index · TG-FTIR · Kinetics

Introduction

Oil shale is a widely recognized resource poised to replace or supplement conventional oil and gas production [1]. However, the semi-coke generated in the refining distillation process has a calorific value of $2500\text{--}4000 \text{ kJ kg}^{-1}$ and is associated with a significant emission. Semi-coke occupies a lot of land, and the leachate produced by semi-coke contains phenolic and sulfur compounds, hydrocarbons, polycyclic aromatic hydrocarbons and various trace metals, thus causing significant environmental damage. This has become an important problem for the development and utilization of oil shale [2, 3]. At present, biomass represents China's fourth largest energy resource, preceded only by coal, oil, and natural gas. Compared with the conventional fossil fuels, it is characterized that C, N, S, and ash content is low. So the CO_2 emission from biomass is far lower than that from fossil fuels. However, most of them are burned directly, during which a lot of energy is wasted and there are increased emissions of pollutant gases and dust particles [4].

There are certain shortcomings when the oil shale semi-coke and corn straw are used as fuel alone. Due to low volatile content, the oil shale semi-coke does not burn

✉ Hongpeng Liu
hongpeng5460@126.com

¹ Engineering Research Centre of Oil Shale Comprehensive Utilization, Ministry of Education, School of Energy and Power Engineering, Northeast Dianli University, Jilin 132012, Jilin Province, China

easily and has other deficiencies. For this reason, it should not be used as a single source for fuel combustion. If corn straw is burned alone, it would produce many gas pollutants, and would cause furnace slagging and wall corrosion [5]. Oil shale semi-coke and corn straw mixed combustion has the advantage of producing fewer harmful substances, thus reducing toxic gases and the wall heating surface corrosion of alkali metal due to fly ash and SO_2 in flue gas when corn straw is used in combustion alone [6, 7]. Meanwhile, biomass combustion processes with zero CO_2 emission are of great interest, in order to address growing environmental concerns and to achieve sustainable development. Co-combustion kinetic analysis can provide theoretical support for combustion in a fluidized bed boiler. The method of co-combustion by the oil shale semi-coke and corn straw not only makes the biomass resource utilization, also reduces the oil shale semi-coke pollution to the environment and uses the heat of semi-coke. So this is low-cost, low-risk way of renewable energy. It has important implications for reducing fossil energy consumption and reducing emissions of SO_2 , NO_x , and CO .

In this paper, we apply thermal gravimetric analysis (TG) and Fourier infrared spectrometric analyzer (FTIR) to study the combustion characteristics of mixtures of different blending ratios at the same heating rate. We also study the combustion characteristics of mixtures of semi-coke and corn straw at blending ratio 7:3 at different heating rates. RMS and MR values are used to evaluate the mutual influence of the co-combustion process. The kinetic parameters of the combustion process for the fuel mixtures were calculated by using a distributed activation energy model (DAEM). The activation energy for mixtures of different blending ratios was also analyzed.

Experimental

Sample preparation

The feedstock materials used in this work were a high-volatile corn straw (CS) and oil shale semi-coke (SC). The samples were collected from the city of Huadian, in the Jilin Province of China. Samples were fabricated according to GB474-2008, and different mixtures of the two materials were prepared according to certain requirements. Each sample weighs about 5 ± 0.5 mg. Table 1 shows the proportions that were used and their designated numbers. In

Table 1 Serial numbers and blend proportions

Blending ratio SC:CS	10:0	9:1	8:2	7:3	6:4	5:5	0:10
Sample serial number	S_1	S_2	S_3	S_4	S_5	S_6	S_7

the table, 9:1 indicates that oil shale semi-coke of the sample S_1 mass fraction is 90 %, mass fraction of corn stalk is 10 % and other samples followed by analogy.

Table 2 shows the results of ultimate and proximate analyses, as well as calorific values for samples used in the experiment. As can be seen from the table, the ultimate analyses revealed the high contents of carbon in corn straw (44.12 %), suggesting a high proportion of organic carbon. Also it can be seen from Table 2 that the corn straw (0.69 %) has higher sulfur content than that of the corn straw (0.02 %). The results of proximate analyses are also given in Table 2. The volatile matter in the corn straw (78.08 %) was almost seven times higher than that in semi-coke (11.73 %). On the other hand, corn straw had higher fixed carbon and higher moisture contents in this study. But the corn straw (4.52 %) has the lower ash content than that of the semi-coke (81.75 %). The corn straw produced had the calorific value of $17,167.5 \text{ kJ kg}^{-1}$, which is higher than that of the semi-coke ($3948.8 \text{ kJ kg}^{-1}$), suggesting that the refining distillation process results in further densification of semi-coke.

Description of the device used in the experiments

The device in this study was thermogravimetric analyzer (TGA/DSC1) made in Switzerland by the biotechnology company METTLER-TOLEDO. The samples were heated from 323 to 1223 K, using heating rates of 10, 20, 40, and 80 K min^{-1} . The carrier gas was dry air with a total gas flow rate of 50 mL min^{-1} . The heat balance was set automatically. The gas emission products from the co-combustion of the samples were determined by coupled with Fourier transform infrared measurements. Evolved gases from the TG pass through a heated transferred line into a beam conforming flow cell in the FTIR sample compartment, and FTIR spectra were collected and stored for further processing. FTIR spectra were collected with 4 cm^{-1} resolution, in the range of $4000\text{--}400 \text{ cm}^{-1}$ IR absorption band. The experimental data were recorded and used to plot co-combustion curves.

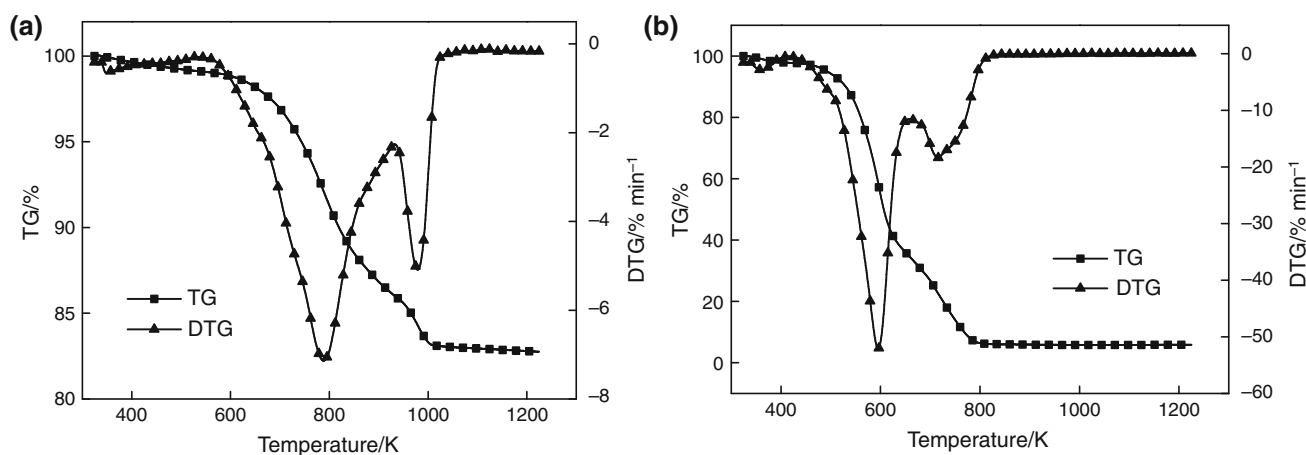
Analytical results of co-combustion

Combustion behavior of individual fuels

Figure 1 shows combustion curves for oil shale semi-coke and corn straw, when a heating rate of 40 K min^{-1} is used. Fig. 1 demonstrates that the combustion rate of oil shale semi-coke is low throughout the entire process, the combustion process occurs at higher temperatures, the burnout temperature is high, and the residual combustion product is of a larger amount. In contrast, the combustion rate of corn

Table 2 Results of proximate and ultimate analyses of oil shale semi-coke and corn straw

Sample	Proximate analysis, air dried/%		Ultimate analysis, air dried/%		Calorific value/kJ kg ⁻¹	
Semi-coke	Carbon	10.65	Moisture	1.18	Qnet,ar	3948.8
	Hydrogen	0.83	Volatile	11.73		
	Oxygen	4.48	Ash	81.75		
	Nitrogen	0.42	Fixed carbon	5.34		
	Sulfur	0.69				
Corn straw	Carbon	44.12	Moisture	6.17	Qnet,ar	17,167.5
	Hydrogen	5.18	Volatile	78.08		
	Oxygen	39.25	Ash	4.52		
	Nitrogen	0.74	Fixed carbon	11.23		
	Sulfur	0.02				

**Fig. 1** TG and DTG curves under heating rate of 40 K min⁻¹ for: **a** oil shale semi-coke and **b** corn straw

straw is high throughout the entire process, the combustion takes place at a relatively low temperature, the burnout temperature is low, and there is a smaller amount of residual combustion product.

Oil shale semi-coke

Figure 1a shows the combustion curves for oil shale semi-coke. According to the thermal gravimetric (TG) and differential thermal gravimetric (DTG) curves, the combustion process of oil shale semi-coke can be divided into three distinct stages. The first stage is the period of loss of water. Because the water content in semi-coke is low, the peak of water mass loss is not obvious. The second stage marks the separation of volatile components and fixed carbon, which occurs in the temperature range 673–933.5 K. Because the volatile and fixed carbon contents in semi-coke are 11.73 and 5.34 %, while the ash content is much higher at 81.75 %, the presence of that much ash represents an obstacle to oxygen diffusion into the fuel particles during the combustion

process. This is not conducive to the combustion of volatile and fixed carbon, so the process of volatile combustion is postponed. The third stage is characterized by a decomposition leading to mineral precipitation, in the temperature range 933.5–1049 K. Because the precipitation of minerals needs higher temperatures, Fig. 1a indicates which minerals are decomposed at temperatures exceeding 933.5 K. Therefore, the burnout of the whole combustion process is delayed, until the temperature reaches 1049 K.

Corn straw

Figure 1b shows the combustion curves for corn straw. According to the TG and DTG curves, the combustion process of corn straw can be also divided into three distinct stages. The first stage is the period of water loss. The moisture in corn straw is higher than that in semi-coke, so the mass loss peak is relatively obvious. The second stage is characterized by the separation of volatile components in the temperature range 509.8–663.9 K [8]. Because the

volatile content in corn straw is 78.08 % and that of ash is 6.17 %, oxygen can easily diffuse into the fuel particles through the ash, so the combustion process is strengthened, and the release of volatile components is violent. The third stage represents the precipitation of fixed carbon in the temperature range 663.9–827.2 K [9]. Because the corn straw contains large amounts of fixed carbon and the process of decomposition of volatile elements releases a large amount of heat, an increase in the fixed carbon combustion peak and burning rate is observed [10].

Segmentation of the TG and DTG curves

Figure 2 shows ignition and burnout temperatures, as well as the combustion process for a mixture of oil shale semi-coke and corn straw, with a blend ratio of 7:3 (sample S_4 in Table 1). Fig. 2 shows that the combustion process can be divided into water loss, low-temperature (ignition temperature T_i – 667 K), transition (667–911.5 K) and high-temperature (911.5 K—burnout temperature T_h) sections. The maximum mass loss rate observed for the combustion peak is $(dw/dt)_{max}$, and the temperature of combustion at which the maximum mass loss rate occurs is T_{max} . The ignition temperature is obtained mostly through TG–DTG extrapolation [11]; details are shown in Fig. 2. The ignition temperature reflects the ignition performance of the blended fuels, activation energy level, and the degree of difficulty with which the fuel starts burning during the reaction; the lower the temperature, the more easily the ignition occurs. The maximum mass loss rate and the corresponding temperature at which it occurs reflect subsequent combustion and burning characteristics of the blended fuels. The greater the value of $(dw/dt)_{max}$, the lower T_{max} , thus indicating that the burning speed following the ignition is faster, and the combustion stability of the blended fuels is stronger.

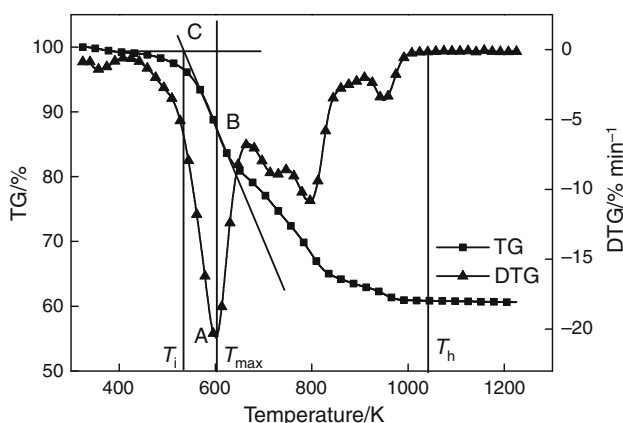


Fig. 2 Schematic representation showing the ignition point, burnout point, and various combustion stages for sample S_4

TG–DTG curves for the combustion of mixtures

Figure 3 shows TG and DTG curves for the mixed fuels of different blending ratios at a heating rate of 40 K min^{-1} . When the proportion of corn straw increases, the combustion of the samples exhibits the tendency to occur at lower temperatures. The temperatures of ignition and burnout decrease, and the segments in the curves marking the volatile mass loss become more obvious. This analysis illustrates that a significant interaction between the oil shale semi-coke and corn straw takes place when they are mixed. According to the TG and DTG curves shown in Fig. 3, co-combustion process of the blending can be divided into four distinct stages. The first mass loss stage is characterized by dehydration, which starts at the point where the TG curve begins to decline, while the DTG curve shows a minimum. The mass loss of the sample is small at this stage. Because corn straw contains more water than the oil shale semi-coke, when the proportion of corn straw increases, the first phase is marked by an increasingly faster decline in the TG curve and a minimum in the DTG curve that gradually reaches lower values. The second, more significant minimum in the DTG curve, marks the second stage in the combustion process when volatiles in the corn straw escape. Since there are a large number of volatiles in corn straw, a more serious mass loss occurs in the sample, which increases as the proportion of corn straw in the blend increases. The third minimum marks the stage of the combustion process related to the fixed carbon in the corn straw and volatiles in the oil shale semi-coke. The fourth minimum marks the decomposition of minerals, since the oil shale of Huadian has a relatively high mineral content. Because minerals in oil shale do not get decomposed and precipitated in the retorting process, they remain mostly in the semi-coke. In the final stage of burning, when the temperature reaches a certain level in the combustion process, the minerals in the semi-coke decompose and precipitate. The mineral content of corn straw is very low, so it almost has no effect on the combustion process of blends with semi-coke. When oil shale semi-coke containing a large number of minerals burns, the minerals decompose and precipitate, which results in minimum in the DTG curve that marks mass loss associated with the final stage of combustion. With increasing proportion of corn straw, the amount of minerals in the mixture decreases, resulting in decreasing mass loss associated with decomposition of minerals. The combustion process of corn straw alone almost does not show any fourth minimum in the DTG curve, due to its insignificant mineral content.

Figure 3a shows that the TG curves of the mixtures become closer to the TG curve for corn straw alone as the proportion of corn straw increases [12]. With increasing

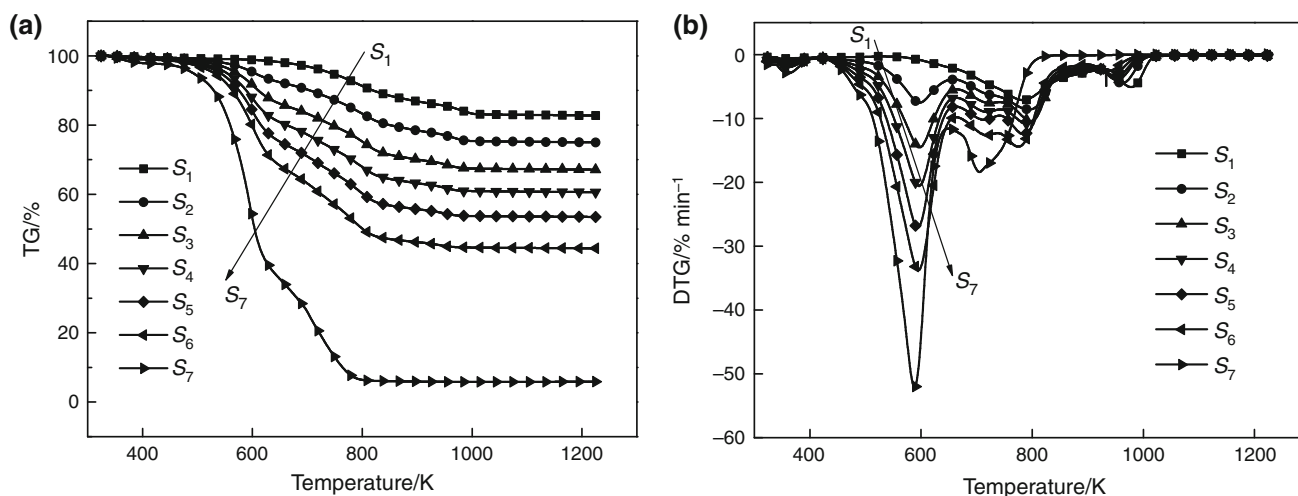


Fig. 3 TG (a) and DTG (b) curves for SC/CS mixtures under heating rate of 40 K min⁻¹

proportion of corn straw, the temperatures at which mass loss occurs and the temperature of devolatilization both decrease. The amount of the non-combustible part of the ash is inversely proportional to the amount of the added corn straw [13]. Therefore, the co-combustion characteristics of the mixtures of oil shale semi-coke and corn straw fall between those of the two individual fuels.

The DTG curves show that the overall mass loss is the lowest when oil shale semi-coke is burned alone, increases when the proportion of corn straw increases and is the largest when corn straw is burned alone. The combustion temperature where maximum mass loss occurs decreases with the increase in proportion of the corn straw. In general, the relative amount of corn straw in the mixtures is proportional to the maximum mass loss rate and is inversely proportional to the temperature of maximum mass loss. Thus, mixing oil shale semi-coke with corn straw increases the reactivity of the oil shale semi-coke. Therefore, this analysis illustrates that a significant interaction between oil shale semi-coke and corn straw occurs when the two fuels are mixed [14, 15].

Table 3 shows the characteristic parameters, which were obtained during co-combustion of corn straw with oil shale semi-coke. The table shows that the ignition temperature and the volatile release temperature decrease when corn straw is added. The reason is that corn straw has a higher reactivity than oil shale semi-coke, and its volatile release starts at a lower temperature. Moreover, the reduction of the temperature of volatile release is proportional to the amount of corn straw in the blend. The significant interaction between oil shale semi-coke and corn straw results in a decrease in the volatile release temperature with increase in the proportion of corn straw in the blend. When the blending ratio of semi-coke to corn straw is 9:1, the ignition temperature of the mixed fuel is reduced to

547.9 K, which is 418.9 K lower than the ignition temperature of semi-coke alone. For blends with a higher proportion of corn straw, the ignition temperature decreases only slightly compared with ratio 9:1, due to the fact that the semi-coke surface is surrounded by highly active corn straw, which reduces the amount of oxygen on the surface of oil shale semi-coke, thus influencing the ignition temperature of the mixed fuels [16]. When blend fuel is combusted, the combustion rate of the highly active corn straw is high. It consumes a lot of oxygen during the combustion process, thus reducing the amount of oxygen on the surface of the less active semi-coke. Also, the presence of more volatiles hinders the diffusion of oxygen to the surface of semi-coke, which leads to a delay of the ignition too.

Compared with the burning of oil shale semi-coke alone, the maximum mass loss temperature (T_{\max}) for a mixture with corn straw is low, indicating that the added corn straw significantly improves the performance of the semi-coke, but the effect is not linear with the proportion of corn straw in the blend. The maximum mass loss temperature for all blends is hovering around 603 K. Similarly, an improvement in the burnout and stability of the corn straw/semi-coke blends is observed compared to combustion of semi-coke alone. In general, it is expected that a highly active fuel, such as corn straw, could improve the burnout of oil shale semi-coke and maintain the stability of the combustion process, due to the difference in their levels of reactivity. Any improvement in the burnout of the less reactive component depends on the oxygen and temperature profiles of the reactor. In the later stages of combustion, the surface of the oil shale semi-coke is surrounded by large amounts of combustion products and ash, which reduce the oxygen and temperature on its surface, thus reducing the degree of burnout. Similar to the maximum mass loss temperature,

Table 3 Combustion characteristics of the various samples under heating rate of 40 K min^{-1}

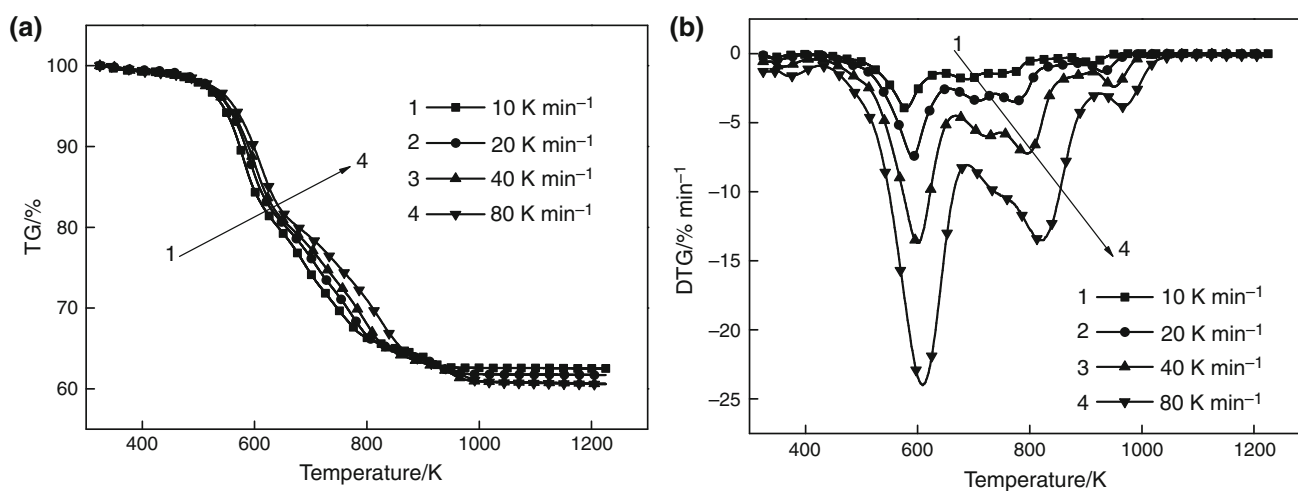
Sample	T_i/K	T_b/K	T_{\max}^1/K	$(dw/dt)_{\max}^1/\% \text{ min}^{-1}$	T_{\max}^2/K	$(dw/dt)_{\max}^2/\% \text{ min}^{-1}$
S ₁	693.8	1069.9	787.4	7.13	978.0	5.08
S ₂	547.9	1061.4	605.8	7.50	798.9	8.58
S ₃	546.7	1036.9	603.9	14.5	800.9	10.4
S ₄	545.9	1017.1	602.2	20.4	796.4	10.8
S ₅	545.8	1014.9	601.9	27	792.2	12.4
S ₆	543.9	1009.8	600.2	33.7	785.5	14.4
S ₇	545.5	843.9	593.1	52	716.9	18.3

the burnout temperature of the mixed fuel does not show a linear relationship with the amounts in the blend. Therefore, this reduces the incremental effect of improvement in the burnout, when the proportion of corn straw in the blend increases.

TG–DTG curves for sample S₄ under various heating rates

To evaluate the influence of the heating rate on the co-combustion of corn straw and semi-coke, we randomly selected sample S₄. Figure 4 shows the TG and DTG curves for this sample at heating rates of 10, 20, 40, and 80 K min^{-1} . As can be seen from Fig. 4, at lower heating rate, the DTG curve shows four distinct minima, which correspond to water loss, volatile release, fixed carbon combustion, and combustion of the minerals in semi-coke. At higher heating rates, the DTG curve gradually starts manifesting only three separate minima. This is due to the water loss of the process being slower at lower heating rates, while there is a lot of loss of water over a short period of time at high heating rates, and the minimum associated

with it is more prominent in the DTG curve. At high heating rates, the rapid precipitation of volatile components and the release of a large amount of combustion heat are associated with the rapid increase in the amount of fixed carbon and the temperature of mineral release. This improves ignition of the minerals. While the heating rate is relatively low, there is less volatile precipitation, and the heat released by the volatile combustion is not sufficient to promote the ignition of the fixed carbon and minerals. As the heating rate increases, the initial temperature of precipitation increases, and the total mass loss rate of the sample also increases, with the largest increase occurring at the most prominent minimum of the DTG curve. Meanwhile, similar to the maximum mass loss rate, the combustion minimum has the tendency to migrate toward higher temperatures; thus, the degree of burnout of the mixed fuel worsens. Among other factors, this is due to the small temperature gradient between the inner and outer surfaces of the mixed fuel at a low heating rate and the easier precipitation of volatiles [17]. Also, oxygen escapes through the pores across the surface of the ash particles, which is conducive to combustion of the volatiles and fixed

**Fig. 4** TG (a) and DTG (b) curves of sample S₄ under various heating rates

carbon, thus increasing the likelihood of a burnout in the presence of sufficient amounts of oxygen. However, at high heating rates, it is just opposite; the result is a shorter combustion time of the blended fuel. Also combustion under those circumstances is more difficult, and a portion of the blended fuel fails to combust fully [18]. Therefore, the heating rate has an important effect on the process of the mixed combustion.

In addition, Table 4 shows that when the heating rate increases, both the ignition and burnout temperatures significantly increase in TG and DTG curves. In that case, each corresponding minimum in the curve has the tendency to migrate to higher temperatures. This is due to the fact that the transport of materials and energy takes time; this phenomenon is manifested by thermal hysteresis. As the heating rate increases, the temperature hysteresis is greater, the initial temperature is higher, and the reaction temperature range becomes wider. Meanwhile, when the heating rate is higher, the furnace temperature increases from the ignition to the burnout temperature of the mixture, and so a higher burnout temperature is observed.

The mutual influence of mixture combustion

In order to better analysis mutual influence of oil shale semi-coke and corn straw in the co-combustion process, analyze and compare experimental and theoretical values of TG–DTG based on the same temperature process. The calculation formulas of theoretical values of TG and DTG as follows:

$$W_{cal} = x_1 W_1 + x_2 W_2 \tag{3.1}$$

$$\left(\frac{dW}{dt}\right)_{cal} = x_1 \left(\frac{dW}{dt}\right)_1 + x_2 \left(\frac{dW}{dt}\right)_2 \tag{3.2}$$

The formula where: W is the residual mass share of samples at the temperature T , %; x_1 and x_2 are accounted for quality of share of oil shale semi-coke and corn straw, %; $(dW/dt)_1$ and $(dW/dt)_2$, which represent the rate of mass loss of semi-coke and corn straw, % min⁻¹.

Figure 5 shows the experimental and theoretical TG and DTG curves of the samples $S_2, S_3, S_4,$ and S_5 at a heating rate of 40 K min⁻¹. From Fig. 5, the mutual influence exists in the co-combustion process, in order to comprehensive and

rational analysis mutual influence of oil shale semi-coke and corn straw numerically. Ref. [19] through the RMS and MR investigated the mutual influence of mixture combustion. The RMS is the relative error root mean square of experimental and theoretical values, and the MR is the ratio of the mean value of absolute error of experimental and the theoretical values. Therefore, this paper evaluates the mutual influence of the co-combustion process by two evaluation parameters. The mutual influence is studied from the two evaluation parameters: The RMS can generally reflect the degree of mutual influence, the larger RMS shows that the interaction between semi-coke and corn straw in th co-combustion process is bigger, and the method comprehensively analyzes the degree of dispersion of experimental value and the theoretical value; MR is used to judge whether the mixed combustion method is conducive to combustion: when $MR > 0$, the two kinds of fuel promote each other in the co-combustion process, and when $MR < 0$, the two kinds of fuel mutually inhibit. RMS and MR are calculated as follows:

$$RMS = \sqrt{\frac{\sum_{i=1}^n \left(\frac{x_{exp}^i - x_{cal}^i}{x_{cal}^i}\right)^2}{n}} \tag{3.3}$$

$$MR = \frac{\sum_{i=1}^n (x_{exp}^i - x_{cal}^i)}{n x_{cal}^{mean}} \tag{3.4}$$

where: x_{exp}^i is the experimental value of the i point, x_{cal}^i is the theoretical value of the i point, x_{cal}^{mean} means the average of the theoretical value, n is the number of points taken from the experiment.

Synergistic effect of different blending ratios

In Fig. 6, the RMS and MR values of the mixed samples with different ratios and different combustion stages at heating rate of 40 K min⁻¹ are given. From Fig. 6a, it is known that the mixture in the second, third, fourth stage have more intense interaction, and the water escape has little effect. And from Fig. 6b, it is known that the beneficial effects mainly occur in the second and the third stage in the co-combustion process, and adverse effects occurred mainly in the fourth stage of the decomposition of minerals

Table 4 Combustion characteristics for sample S_4 under various heating rates

Heating rate/K min ⁻¹	T_i /K	T_b /K	T_{max}^1 /K	$(dw/dt)_{max}^1$ /% min ⁻¹	T_{max}^2 /K	$(dw/dt)_{max}^2$ /% min ⁻¹
10	532.2	970.0	528.1	3.98	691.5	1.84
20	540.1	1001.5	605.2	7.47	777.5	3.47
40	545.9	1017.1	602.2	13.7	796.4	7.23
80	551.6	1058.6	610.9	23.9	820.8	13.5

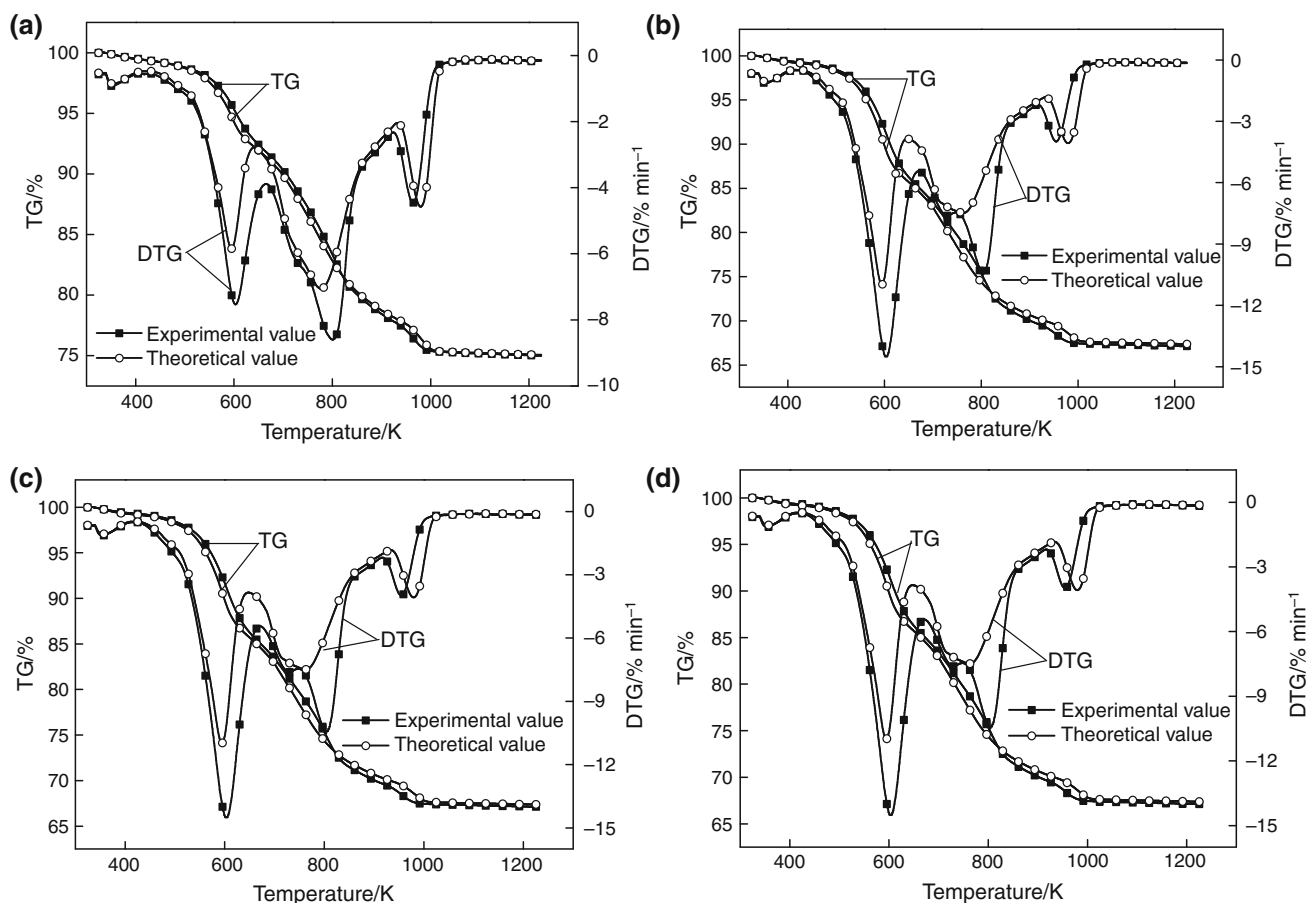


Fig. 5 Comparison of TG and DTG experimental curves and theoretical curves of different mixtures for **a** S_2 ; **b** S_3 ; **c** S_4 ; **d** S_5

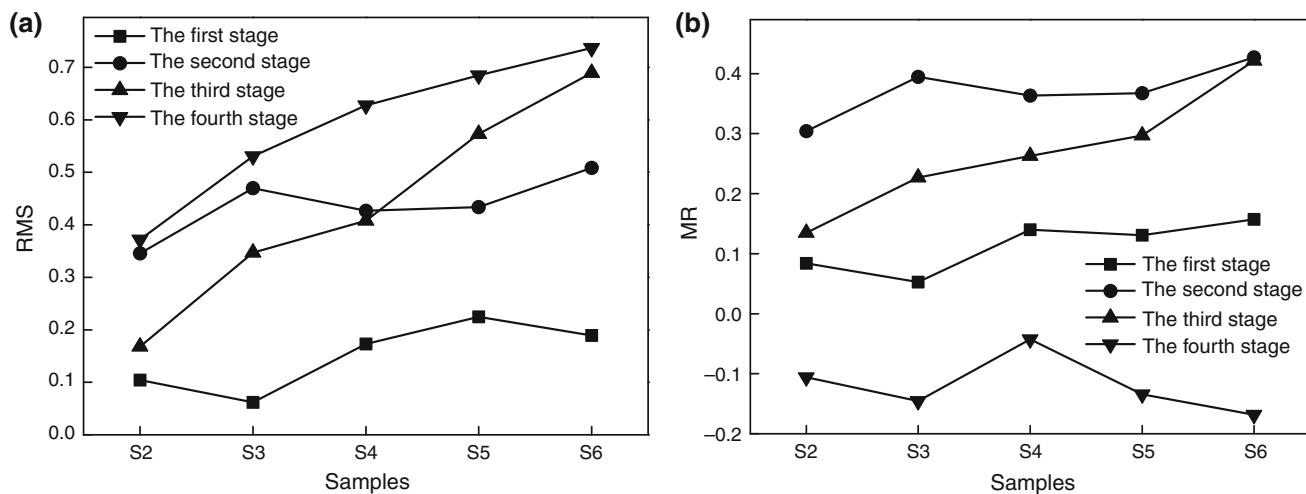


Fig. 6 RMS and MR indices of co-combustion samples for **a** RMS; **b** MR

of oil shale semi-coke; only two kinds of fuel in sample S_4 promote each other. The reason for this phenomenon is that when the corn straw ratio is too small, due to the lower calorific value of semi-coke, heat release of the mixture

during the previous stages of combustion is less; the two fuels appear mutual “compete” heat in the subsequent ignition and combustion process. When the proportion of corn straw is too large, because of the organic matter of

corn straw is more, more oxygen is expended, resulting in two kinds of fuel “compete” oxygen in the co-combustion process with each other. Whether lack of heat when corn straw is too small, or lack of oxygen when the ratio is too large, will lead to poor co-combustion effect, manifested as corn straw and semi-coke mutual inhibition. When the mass ratio of oil shale semi-coke and corn straw is 7:3, the mutual influence is the largest and the beneficial effects on the whole progress, it can improve the combustion characteristics of the two fuels.

Synergistic effect of different heating rates

Figure 7 shows the mutual influence index RMS and MR value of sample S_4 in different combustion stages at heating rate of 10, 20, 40, and 80 K min^{-1} . It can be seen from Fig. 7, the mixed samples in the first stage which the water escape section is almost no effect, the later three stages have intense interaction in the co-combustion process, which the second and third stages are beneficial, and the fourth stage is adversely effected. When the heating rate is 20 K min^{-1} , the interaction of oil shale semi-coke and corn straw has the greatest influence and is beneficial to promote the combustion of the two fuels and improve the combustion characteristics of the fuel.

FTIR analysis of gas products

Figure 8 shows the FTIR of the S_1 , S_3 , S_4 , S_7 at a heating rate of 40 K min^{-1} . From Fig. 8a can be seen, the combustion gaseous products of oil shale semi-coke are mainly CO_2 , CO , H_2O . The gaseous products of semi-coke is very few. Figure 8d shows the combustion gaseous products of corn straw in addition to CO_2 , CO , and H_2O , at the early

stage of the reaction, at the 610–740 cm^{-1} appeared the obvious peak caused by O–H and C–H out of plane bending vibration, at the 1000–1200 cm^{-1} appeared C–H in-plane bending vibration, C–C, C–O bond skeleton vibration peak, at the 1600–1850 cm^{-1} appear the C=C and C=O double-bond stretching vibration peak, corresponding to various alcohols and phenols, carboxylic acids, ketones, aldehydes, and other macromolecular materials [20]. Figure 8b, c shows that the co-combustion process of oil shale semi-coke and corn straw mixture with single semi-coke is obviously different, with the increase in corn straw in the mixture, the gaseous products and the quantity of the gas are more and more close to the corn stalk, and burnout rate is improved, indicating that join the addition of corn straw could improve the combustion properties of the mixture, consistent with the above TG results.

FTIR analysis for the mixed fuels of different blending ratios

CO_2 and CO release of the mixed fuels in the combustion process are given in Fig. 9; it can be known that the absorption peak of CO in oil shale semi-coke is a wide and high peak, and also absorption peak of CO_2 in corn straw is a wide and high peak. During the co-combustion process, the absorption intensity of CO_2 increases gradually, and the absorption intensity of CO decreases gradually with the proportion of corn straw increase. The change of CO_2 and CO is consistent with the change of DTG curves, this shows that the addition of corn straw can improve burnout characteristics of mixed fuels. In order to analyze the influence of the mass ratio of semi-coke and corn straw to the CO_2 and CO release in the combustion process, and then analyze the burnout rate of the mixtures by $A_{\text{CO}}/A_{\text{CO}_2}$. Based on the line $y = 0$ as the baseline, the CO and CO_2

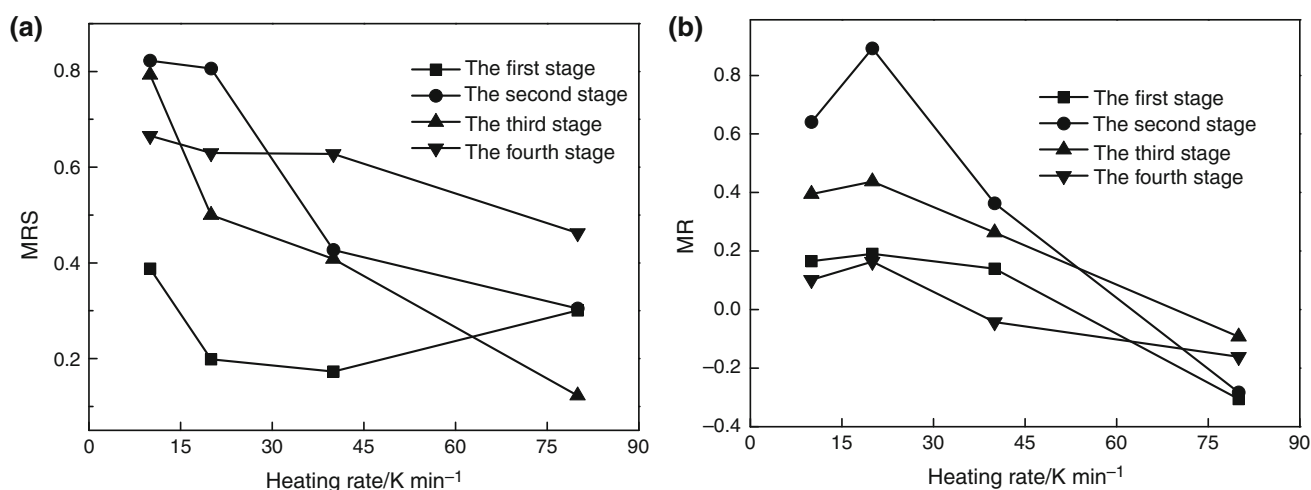


Fig. 7 RMS and MR index of sample S_4 for a RMS; b MR

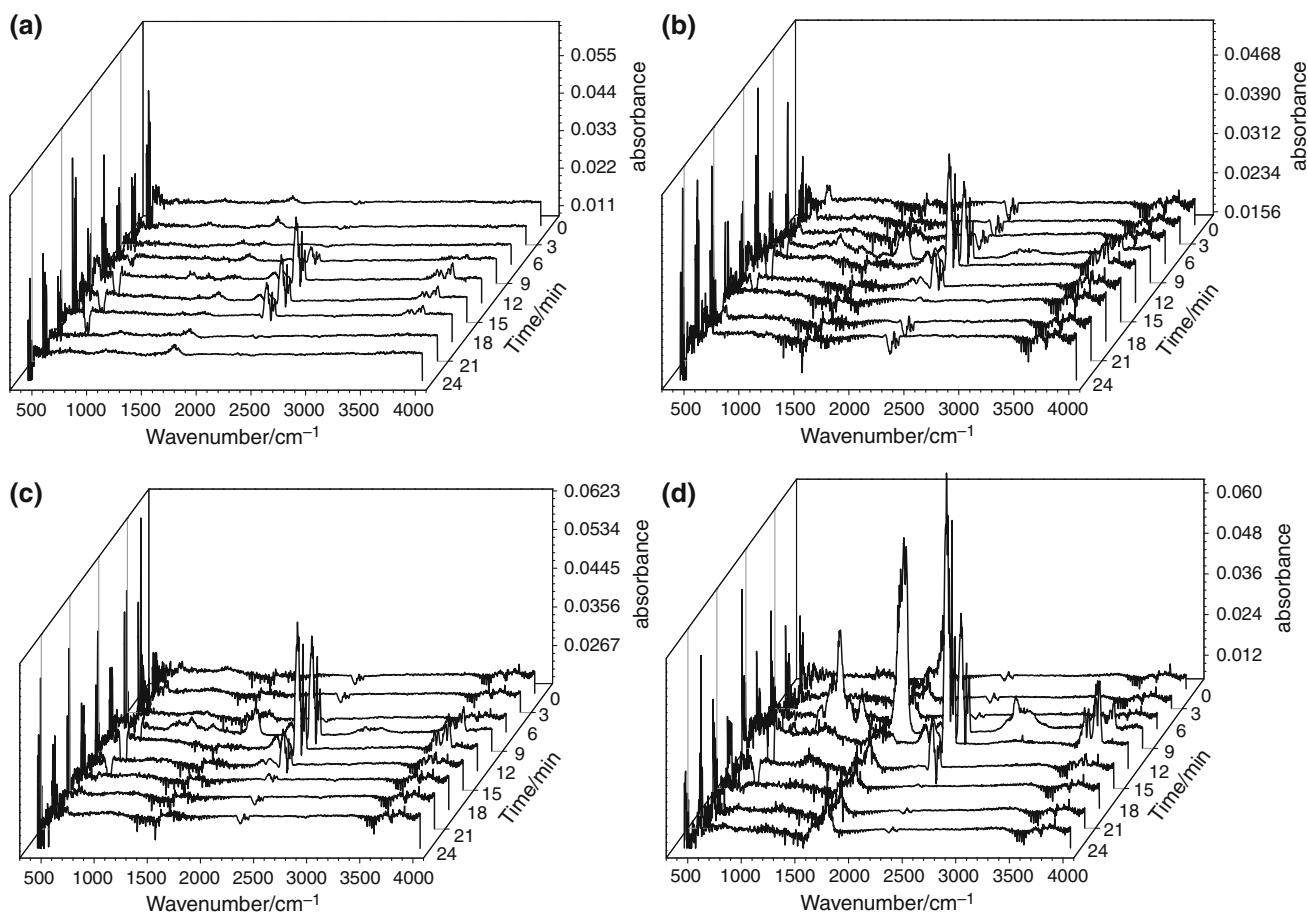


Fig. 8 FTIR spectrum of semi-coke, corn straw, and their mixtures combustion for **a** S_1 ; **b** S_3 ; **c** S_4 ; **d** S_7

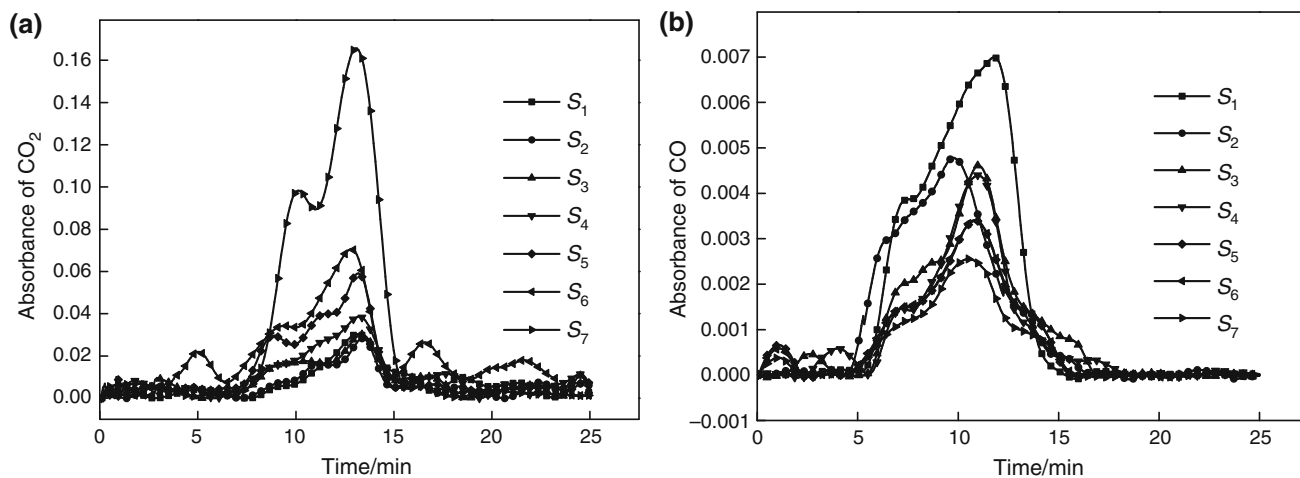


Fig. 9 CO_2 and CO release rules of the mixtures under heating rate of 40 K min^{-1} for **a** CO_2 ; **b** CO

absorbance curves are integral to the baseline, and the area of the integral is approximated as the CO and CO_2 released by the combustion process; the area is represented by A_{CO} and A_{CO_2} , respectively. The $A_{\text{CO}}/A_{\text{CO}_2}$ represents the

burnout rate of the mixtures. Table 5 shows that, with the increase in mass ratio of corn straw, $A_{\text{CO}}/A_{\text{CO}_2}$ gradually decreases, indicating the proportion of CO is less and less, proportion of CO_2 is more and more, more and more semi-

Table 5 Data comparisons of FTIR at various samples

Parameters	S_1	S_2	S_3	S_4	S_5	S_6	S_7
A_{CO}	0.038	0.028	0.023	0.021	0.019	0.019	0.014
A_{CO_2}	0.191	0.162	0.209	0.262	0.323	0.491	0.727
A_{CO}/A_{CO_2}	0.199	0.173	0.110	0.080	0.059	0.039	0.019

coke in the mixtures is burned, so as to improve burnout rate of mixed fuels. Therefore, the co-combustion of semi-coke and corn straw can not only reduce the air pollution, but also can effectively improve the efficiency of the mixed fuels.

FTIR analysis for sample S_4 under various heating rates

Figure 10 shows the variation of CO_2 and CO of S_4 with time at different heating rates. Based on the line $y = 0$ as the baseline, the CO and CO_2 absorbance curves are integral to the baseline, and the area of the integral is approximated as the CO and CO_2 released by the combustion process and the results are shown in Table 6. With the increase in heating rate, the CO_2 , CO precipitation peak gradually moves to the left, the end time of the release is significantly earlier, and the width of the absorption peak of CO_2 and CO has a narrowing trend. That is, with the increase in heating rate, the release time of gaseous products is shorten, which is favorable for the combustion reaction. From Table 6 we can see that, with the increase in heating rate, A_{CO_2} and A_{CO} gradually decrease, but the A_{CO}/A_{CO_2} first decreases and then increases, and the value of A_{CO}/A_{CO_2} is minimum at the heating rate of 20 K min^{-1} . That the heating rate is 20 K min^{-1} , combustion effect of mixed fuels is best, and the burnout rate is highest.

Co-combustion kinetic analysis

At present, the energy analysis of distributed and independently combusted fossil fuel is often carried out using the model of distributed activation energy (DAEM). For the sake of better understanding, the multistep reaction mechanism of combustion kinetics, the relationship between activation energy (E) and conversion degree (α) is evaluated for different heating rates, using the iso-conversional method. The solution in this paper is based on the integral method proposed by Miura [21].

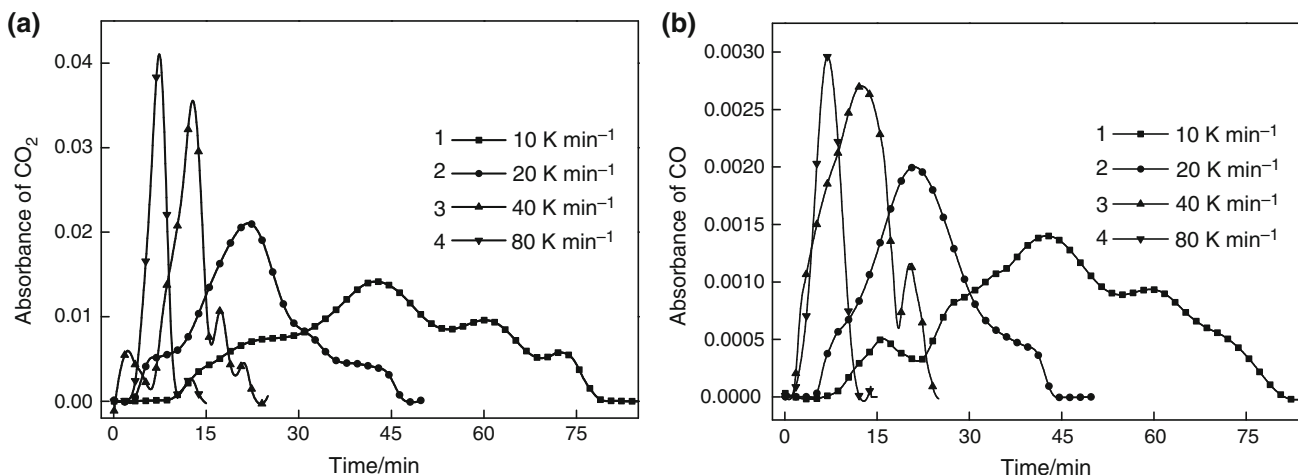
The model assumes that many irreversible first-order parallel reactions that have different rate parameters occur simultaneously. When the model is used to analyze co-combustion of corn straw and semi-coke, change in the total volatiles, V , against time, t , is given by

$$1 - \frac{V}{V^*} = \int_0^{\infty} \exp\left(-A \left(\int_0^t e^{-E/RT} dt\right)\right) f(E) dE \quad (5.1)$$

where V^* denotes the total volatile component of the fuel in the reaction process, and let V marks the volatiles produced by V^* at a certain time. $f(E)$ is the activation energy distribution function and satisfies Eq. (5.2). A is the frequency factor corresponding to the E value.

Table 6 Data of FTIR at different heating rate

Parameters	Heating rate/ K min^{-1}			
	10	20	40	80
A_{CO}	0.057	0.038	0.031	0.016
A_{CO_2}	0.543	0.396	0.292	0.143
A_{CO}/A_{CO_2}	0.105	0.096	0.106	0.112

**Fig. 10** CO_2 and CO release rules of sample S_4 under various heating rates for **a** CO_2 ; **b** CO

$$\int_0^{\infty} f(E) dE = 1 \quad (5.2)$$

$$\Phi(E, T) = \exp\left(-A \int_0^t e^{-E/RT} dt\right) \quad (5.3)$$

To simplify Eq. (5.1), the so-called Φ function in Eq. (5.1) was approximated by a step function at $E = E_s$, where β is a constant heating rate. Equation (5.1) was then simplified to Eq. (5.4):

$$\frac{V}{V^*} \cong 1 - \int_{E_s}^{\infty} f(E) dE = \int_0^{E_s} f(E) dE \quad (5.4)$$

The activation energy, E_s , was chosen to satisfy $\Phi(E_s, T) = 0.58$. The relationship of E_s , to β , T , and A is given by

$$\frac{0.545\beta E_s}{ART_2} = e^{-E_s/RT} \quad (5.5)$$

with the following approximate equation for $\Phi(E, T)$:

$$\Phi(E, T) \cong \exp\left(-\frac{ART^2}{\beta E} e^{-E/RT}\right) \quad (5.6)$$

The approximation is given mathematically by

$$\frac{dV}{dt} \cong \frac{dV}{dt} = Ae^{-E/RT}(\Delta V^* - \Delta V) \quad (5.7)$$

Where ΔV^* is the effective volatile volume of the reaction, generated in the activation energy range E to $E + \Delta E$, and ΔV is the volatile component that escapes from V^* at any given time: With β as constant, according to Miura's integral method [22], Eq. (5.7) can be rewritten as follows:

$$1 - \frac{\Delta V}{V^*} = \exp\left(-A \int_0^t e^{-\frac{E}{RT}} dt\right) \cong \exp\left(-\frac{ART^2}{\beta E} e^{-E/RT}\right) \quad (5.8)$$

Equation (5.8) is rewritten

$$\ln\left(\frac{\beta}{T^2}\right) = \ln\left(\frac{AR}{E}\right) - \ln\left\{-\ln\left(1 - \frac{\Delta V}{V^*}\right)\right\} - \frac{E}{RT} \quad (5.9)$$

A step function at $E = E_s$ is used to simplify Eq. (5.9), and E_s satisfies $\Phi(E_s, T) = 0.58$; Eq. (5.9) then can be simplified to

$$\ln\left(\frac{\beta}{T^2}\right) = \ln\left(\frac{AR}{E}\right) + 0.6075 - \frac{E}{RT} \quad (5.10)$$

Plot $\ln(\beta/T^2)$ against $1/T$ at the selected conversion degree, and the E and A values can be obtained from the

slope and the intercept in each Arrhenius plot. At the same time, the activation energy distribution curve ($E - \alpha$) can be obtained. The activation energy curves for several different blending ratios are shown in Fig. 11.

The degree of difficulty for the reaction to occur is represented by the activation energy. As can be seen from Fig. 11, the activation energy of oil shale semi-coke (sample S_1) is increasing with the conversion degree. E values gradually went from 148.50 to 454.39 kJ mol^{-1} . Since the flammable volatiles of oil shale semi-coke are the first to combust, less energy is required, and the activation energy is low. When the volatile components are burned at low temperature, the reaction becomes more difficult, and the activation energy increases with the increase in the amounts of fixed carbon and minerals at the late reaction stage. In the combustion process of corn straw (sample S_7), the activation energy increases firstly and then decreases. As α increase from 0.02 to 0.60 represented the oxidative pyrolysis of volatiles, E values gradually increase from 193.77 to 393.40 kJ mol^{-1} , and E values gradually increase from 393.40 to 261.58 kJ mol^{-1} when the conversion degree range of 0.60–1.0. This is due to the corn straw containing a large amount of volatile matter. For this reason, it produces a lot of heat when it is burned, so that the combustion continues with high intensity; hence, the activation energy decreases at the late stage of the reaction.

From Fig. 11, we can see that the corn straw is more prone to reaction than the oil shale semi-coke. At the late stage of the reaction in particular, the mineral content of corn straw is low, making it easier to burn. With the proportion of corn straw in the blend increasing, the activation energy decreases, and the reaction of the mixture components becomes more likely to occur, indicating an obvious effect of the co-combustion of oil shale semi-coke and biomass. Overall, with the proportion of corn straw rising

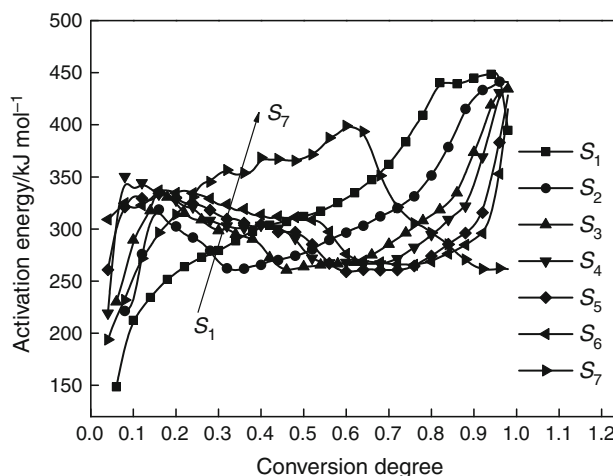


Fig. 11 Activation energy versus conversion degree

in the blends, the activation energy shows a downward tendency, due to the fact that corn straw contains more volatiles and the volatile combustion can generate a lot of heat. This promotes the ignition of fixed carbon and minerals. It has been reported that the property of volatiles for the sample would affect the E values, for instance, the chemicals wastewater and lignite [23], oil-palm solid wastes, and paper sludge [24]. When the blending ratio of semi-coke to corn straw is 7:3, the average value of the E is minimum, which is $307.43 \text{ kJ mol}^{-1}$. So sample S_4 was potentially an optimal option for the combustion of the blends, which made it more available for the whole combustion process. Similar results are found in the literature [25], when the blending ratio of paper sludge and rice straw is 8:2, the average value of the E attained the minimum, which was 132 kJ kg^{-1} . This result might be caused by the interaction between semi-coke and corn straw during the combustion process. This effect has been studied [24]. Therefore, the combustion process of the mixtures containing corn straw becomes accelerated, which promotes the reaction. All this confirms the results of the analysis of the DTG and FTIR curves above.

Conclusions

1. The co-combustion process of the mixtures of oil shale semi-coke and corn straw can be divided into water, volatiles in the corn straw, fixed carbon in the corn straw and volatiles in the oil shale semi-coke, and minerals sections.
2. The burning rate of oil shale semi-coke alone is low. Therefore, the combustion in that case requires high temperatures, the burnout temperature is also high, and the combustion process is incomplete, leaving a larger amount of residue. As the percentage of corn straw in the blends increases, the ignition temperature, peak temperature, and burnout temperature tend to decrease. Meanwhile, the maximum and average mass loss rates of the blends increase, which improves to a certain extent the combustion characteristics of mixed fuels.
3. Increase in the heating rate causes the phenomenon of thermal hysteresis. The combustion process shifts toward higher temperatures, while the burning time gets reduced, and burnout of the fuel becomes more difficult. As the heating rate increases, the ignition, peak, and burnout temperatures shift to higher values. Increasing heating rates also result in increase in the maximum and average mass loss rates.
4. There exists mutual influence between oil shale semi-coke and corn straw in the co-combustion, and interaction occurred mainly in the second, the third, and the fourth stage. The second and third stages are

the favorable effects, and the fourth stage is the adverse effect and when corn straw and semi-coke mass ratio of 7:3, the mutual influence on the whole semi-coke and corn straw are the largest and the beneficial effects. In general, the semi-coke and corn straw were mutually inhibited when the proportion of corn stalks in the mixture is too large or too small in the process of mixing.

5. With the increase in corn straw ratio, A_{CO}/A_{CO_2} decreases gradually, more and more oil shale semi-coke of the mixture is burned, improve the utilization rate of fuel. The value of A_{CO}/A_{CO_2} is minimum at the heating rate of $20 \text{ }^\circ\text{C min}^{-1}$, combustion effect of mixed fuels is best, and the burnout rate is highest.
6. The activation energy of oil shale semi-coke at high temperature is larger than that at low temperatures, while the opposite is observed for corn straw. The average activation energy of semi-coke is significantly higher than that for corn straw. When the blending ratio is 7:3 (sample S_4), the average value of the E is minimum, which is $307.43 \text{ kJ mol}^{-1}$. This indicates that a mixed burning effect is obvious for the mixtures of oil shale semi-coke and corn straw.

Acknowledgements This study was supported by the Science and Technology Development Projects of Jilin Province, China (20130522067JH), Science and Technology Development Projects of Jilin city (201467005) and Program for Changjiang Scholars and Innovative Research Team in Universities, China (IRT13052).

References

1. Ma L, Yin XY, Sun H, Fu BS. Present status of oil shale resource utilization in the world and its development prospects. *Global Geol.* 2012;31:772–7 (in Chinese).
2. Triikkel A, Kuusik R, Martins A, Pihu T, Stencil JM. Utilization of Estonian oil shale semi-coke. *Fuel Process Technol.* 2008;89: 756–63.
3. Gusca J, Siirde A, Eldermann M. Energy related sustainability analysis of shale oil retorting technologies. *Energy Procedia.* 2015;72:216–21.
4. Joselin H, Krishnan UA. Quantifying environmental performance of biomass energy. *Renew Sustain Energy Rev.* 2016;59:292–308.
5. Marcus O, Anders N, Bengt-Johan S, Rainer B, Mikko H. Bed agglomeration characteristics during fluidized bed combustion of biomass fuels. *Energy Fuels.* 2000;14:169–78.
6. Xu CX, Mao JX, Zeng RL. Combustion theory and combustion equipment. Beijing: China Machine Press; 1990 (in Chinese).
7. Wang X, Ren QQ, Li LN, Li SY, Lu QG. TG–MS analysis of nitrogen transformation during combustion of biomass with municipal sewage sludge. *J Therm Anal Calorim.* 2016;123:2061–8.
8. Vamvuka D, Salpigidou N, Kastanaki E, Sfakiotakis S. Possibility of using paper sludge in co-firing applications. *Fuel.* 2009;88:637–43.
9. Gil MV, Casal D, Pevida C, Pis JJ, Rubiera F. Thermal behaviour and kinetics of coal/biomass blends during co-combustion. *Bioresour Technol.* 2010;101:5601–8.

10. Stenseng M, Zolin A, Cenni R, Frandsen F, Jensen A, Dam-Johansen K. Thermal analysis in combustion research. *J Therm Anal Calorim.* 2001;64:1325–34.
11. Yu QM, Pang YJ, Chen HG. Determination of ignition points in coal-combustion tests. *North China Electric Power.* 2001;7:9–10, 50 (in Chinese).
12. Magdziarz A, Wilk M. Thermal characteristics of the combustion process of biomass and sewage sludge. *J Therm Anal Calorim.* 2013;114:519–29.
13. Zheng G, Kozinski JA. Thermal events occurring during the combustion of biomass residue. *Fuel.* 2000;79:181–92.
14. Skodras G, Grammelis P, Basinas P. Pyrolysis and combustion behaviour of coal–MBM blends. *Bioresour Technol.* 2007;98:1–8.
15. Zhou LM, Wang YP, Huang QW, Cai JQ. Thermogravimetric characteristics and kinetic of plastic and biomass blends co-pyrolysis. *Fuel Process Technol.* 2006;87:963–9.
16. Grotkjaer T, Dam-Johansen K, Jensen AD, Glarborg P. An experimental study of biomass ignition. *Fuel.* 2003;82:825–33.
17. Zhai YB, Peng WF, Zeng GM, Fu ZM, Lan YM, Chen HM, Wang C, Fan XP. Pyrolysis characteristics and kinetic of sewage sludge for different size and heating rates. *J Therm Anal Calorim.* 2012;107:1015–22.
18. Magdziarz A, Wilk M. Thermogravimetric study of biomass, sewage sludge and coal combustion. *Energy Convers Manag.* 2013;75:425–30.
19. Liu HP. Co-combustion characteristics of oil shale retorting solid waste and biomass [D]. Tianjin University, 2012 (in Chinese).
20. Ganesh KP, Augustine Q, Raghu B, et al. TGA–FTIR investigation of co-combustion characteristics of blends of hydrothermally carbonized oil palm biomass (EFB) and coal. *Fuel Process Technol.* 2014;118:228–34.
21. Miura K. A new and simple method to estimate $f(E)$ and $k_0(E)$ in the distributed activation energy model from three sets of experimental data. *Energy Fuel.* 1995;9:302–7.
22. Miura K, Maki T. A simple method for estimating $f(E)$ and $k_0(E)$ in the distributed activation energy model. *Energy Fuel.* 1998;12:864–9.
23. Chen JB, Lin M, Cai JC, Yin HC, Song XG, Li AM. Thermal characteristics and kinetics of refining and chemicals wastewater, lignite and their blends during combustion. *Energy Convers Manag.* 2015;100:201–11.
24. Lin YS, Ma XQ, Yu ZS, Cao YW. Investigation on thermochemical behavior of co-pyrolysis between oil-palm solid wastes and paper sludge. *Bioresour Technol.* 2014;166:444–50.
25. Xie ZQ, Ma XQ. The thermal behaviour of the co-combustion between paper sludge and rice straw. *Bioresour Technol.* 2013;146:611–8.